



ARTICLE

Enhancing Friction Stir Welding in Fishing Boat Construction through Deep Learning-Based Optimization

Erfan Maleki¹ Okan Unal^{2,3} Seyed Mahmoud Seyedi Sahebari⁴ Kazem Reza Kashyzadeh^{5*}
Nima Amiri⁶

1. Mechanical Engineering Department, Politecnico di Milano, Milan, 20156, Italy

2. Mechanical Engineering Department, Karabuk University, Karabuk, 78050, Turkey

3. Modern Surface Engineering Laboratory, Karabuk University, Karabuk, 78050, Turkey

4. Department of Mechanical and Manufacturing Engineering, Ontario Tech University, L1G 0C5ON, Oshawa, Canada

5. Department of Transport, Academy of Engineering, RUDN University, 6 Miklukho-Maklaya Street, Moscow, 117198, Russian Federation

6. Paul M. Rady Department of Mechanical Engineering, University of Colorado, Boulder, CO, 80309, United States

ARTICLE INFO

Article history

Received: 17 June 2023

Revised: 10 August 2023

Accepted: 18 August 2023

Published Online: 19 August 2023

Keywords:

Simulation and modelling

Welding

Friction stir welding

Deep neural network

Optimization

ABSTRACT

In the present study, the authors have attempted to present a novel approach for the prediction, analysis, and optimization of the Friction Stir Welding (FSW) process based on the Deep Neural Network (DNN) model. To obtain the DNN structure with high accuracy, the most focus has been on the number of hidden layers and the activation functions. The DNN was developed by a small database containing results of tensile and hardness tests of welded 7075-T6 aluminum alloy. This material and the production method were selected based on the application in the construction of fishing boat flooring, because on the one hand, it faces the corrosion caused by proximity to sea water and on the other hand, due to direct contact with human food, i.e., fish etc., antibacterial issues should be considered. All the major parameters of the FSW process, including axial force, rotational speed, and traverse speed as well as tool diameter and tool hardness, were considered to investigate their correspondence effects on the tensile strength and hardness of welded zone. The most important achievement of this research showed that by using SAE for pre-training of neural networks, higher accuracy can be obtained in predicting responses. Finally, the optimal values for various welding parameters were reported as rotational speed: 1600 rpm, traverse speed: 65 mm/min, axial force: 8 KN, shoulder and pin diameters: 15.5 and 5.75 mm, and tool hardness: 50 HRC.

*Corresponding Author:

Kazem Reza Kashyzadeh,

Department of Transport, Academy of Engineering, RUDN University, 6 Miklukho-Maklaya Street, Moscow, 117198, Russian Federation;

Email: kazem.kashyzadeh@gmail.com

DOI: <http://dx.doi.org/10.36956/sms.v5i2.875>

Copyright © 2023 by the author(s). Published by Nan Yang Academy of Sciences Pte Ltd. This is an open access article under the Creative Commons Attribution-NonCommercial 4.0 International (CC BY-NC 4.0) License. (<https://creativecommons.org/licenses/by-nc/4.0/>).

1. Introduction

One of the oldest methods of non-separable connections, which is widely used in various industries, is welding. In fact, large structures cannot be produced in one piece, such as the body of ships, airplanes, trains, subways, and ground vehicles ^[1, 2]. Therefore, it is necessary to connect different parts to each other and create an assembly. Hence, depending on the application of the connection, different types of welding are used in various industries, each of which has advantages and disadvantages compared to the others ^[3]. For example, the biggest challenge for all types of welding methods is the creation of tensile residual stress in the welding area ^[4] or microstructure change in the Heat-Affected Zone (HAZ), both of which lead to a decrease in joint strength ^[5, 6]. In other words, these two areas are prone to damage and cracks. However, some additional disadvantages arise when an intermediate material is used for welding. Therefore, in large industries, it is usually tried to use welding methods that do not require an electrode or additional material, such as Resistance Spot Welding (RSW) in the automotive industry ^[7]. Moreover, the FSW process which was first presented by The Welding Institute (TWI) in 1991 ^[8], has emerged as an effective alternative to traditional Metal Inert Gas (MIG) welding for use in marine applications, particularly as the industry moves towards increased use of aluminum alloys. Based on the TWI report in 2007, 171 large organizations and companies received licenses to manufacture shipbuilding from aluminum extrusion by FSW process, especially, Al7075 is used to manufacture aluminum panels for deep freezing of fishing boats. In this regard, one of the biggest challenges and concerns in the manufacturing is to optimize the strength of welded joints via the welding process. The powerful combination of reduced weight from aluminum and increased strength of FSW welds can yield spectacular benefits for marine designs. Generally, FSW is well suited for marine applications because of the nature of the welds ^[9]. During the last decades, the selection of the favorable parameters of this process to obtain the optimal properties of the welded parts is remained challenging and widely considered by many researchers. In this regard, the goal is to increase the quality and improve the strength of the connection, and for this purpose, various techniques have been used. The number of publications in this field is very large and a comprehensive study is required for a detailed review, which is beyond the scope of the present research. However, some of the efforts made to optimize aluminum parts welded in this way are collected in Table 1.

As presented in Table 1, scientists paid the most atten-

tion to data mining methods such as Taguchi Method (TM), Linear Regression Method (LRM), Analysis of Variance (ANOVA), and Response Surface Method (RSM) to optimize different parameters of FSW process. In addition, the main goal was to improve the tensile strength and hardness of the connection. In recent years, attention has been paid to machine learning methods such as Artificial Intelligence (AI) for modeling and optimizing friction stir welding of aluminum alloys. Nevertheless, the present article includes the most comprehensive laboratory results and six input parameters. Also, the deep machine learning method was used to provide a new approach in optimizing the friction stir welding process of aluminum parts. Recently, the advantages and accuracy of using Deep Neural Network (DNN) technique compared to Artificial Neural Network (ANN) have been evident and proven in various fields of engineering ^[28, 29]. Padhy et al. have published a comprehensive review on the FSW technology and the effects of process parameters on the material characterization and metallurgical properties like microstructure ^[30]. In addition, Gangwar and Ramulu have focused on the titanium alloys joints by FSW ^[31]. Also, to improve the quality of this type of welded joint, the effects of two parameters of the tool and the thickness of the raw material sheets have been evaluated. After that, microstructure, material properties (i.e., hardness), mechanical properties (i.e., tensile, fatigue, and fracture toughness), residual stress field, and temperature distribution have been studied. Mohanty et al. have utilized RSM to examine the effects of tool shoulder and probe profile geometries simultaneously on the FSW of aluminum sheets ^[32]. In this research, three parameters of tool type, tool probe diameter, and shoulder flat surface, each of them at three different levels, were considered as input to the RSM analysis. Also, connection strength, weld cross section area, and grain size in both welded area and HAZ were considered as output. The results showed that straight cylindrical FSW tool with the minimum level of probe diameter provided better strength of welded joint. Ahmed et al. have optimized FSW process parameters to achieve the maximum tensile strength and hardness of welded 5451Al sheets by performing Taguchi sensitivity analysis ^[33]. They stated that the pin profile of the tool is the most effective factor in both outputs with more than 60% effectiveness. Moreover, research on the connection of thick aluminum plates through FSW has also been carried out ^[34]. Before this, in most articles, the connection of thin sheets up to 5 or 6 mm has been considered. In this regard, Kumar et al. have proposed a trapezoidal pin of tool to reach a free-defect connection of 12 mm thick aluminum sheets. constructions, which are ultimately directly or indirectly related to the economic field

and cost. For example, in the construction of a fishing boat, it is possible to refer to the initial costs including the preparation of the raw material i.e., aluminum alloy, the construction design including the dimensions and thicknesses of the sheets for the construction of the ship, and finally the construction method and the type of connection of the sheets to each other. On the other hand, considering the working conditions in the vicinity of sea water and the corrosion as a result, and on the other hand, in direct connection with fish and antibacterial issues, it is necessary to choose the type of alloy and heat treatment correctly.

Finally, in order to reduce production time and ultimately reduce the cost of free-defect production, in order to minimize repairs, it is necessary to optimize the production process. Apart from these cases, just the free-defect construction is not enough, and it must have enough strength so that it does not have problems after some time of use^[35]. For this purpose, in addition to examining the tensile strength, it is better to study the hardness and microstructure in the welded area. Therefore, the results of such research can satisfy part of the demands stated above.

Table 1. A summary of the research conducted to optimize the friction stir welding of aluminum parts.

Reference	Year	Material	Method	Parameters	Objective
[10]	2015	AA6082-T6	Taguchi	Joint geometries: butt, lap, and T-shaped	Ultimate tensile strength
[11]	2010	AA1050	Grey relation analysis and Taguchi	Rotating speed, welding speed, and shoulder diameter	Tensile strength and elongation
[12]	2015	AA8011	Taguchi-Based Grey Relational Analysis	Tool shoulder diameter, rotational speed, welding speed, and axial load	Tensile strength and microhardness
[13]	2016	Cast AA7075/SiCp Composite	Response surface methodology, regression model, and Fuzzy grey relational analysis approach	Spindle speed, travelling speed, downward force, and percentage of SiC added to AA7075	Ultimate tensile strength and percentage elongation
[14]	2019	AA6082/SiC/10P composite	Taguchi approach and analysis of variance (ANOVA)	Tool rotation speed, welding speed, and tool tilt angle	Ultimate tensile strength
[15]	2018	Dissimilar alloys (AA6082/AA5083)	Taguchi method, Grey relational method, weight method, and analysis of variance (ANOVA)	Tool rotation speed, welding speed, tool pin profile, and shoulder diameter	Ultimate tensile strength and elongation
[16]	2008	RDE-40 aluminium alloy	Taguchi technique and analysis of variance (ANOVA)	Rotational speed, traverse speed, and axial force	Tensile strength
[17]	2010	AA7075-T6	Response surface methodology and analysis of variance (ANOVA)	Tool rotational speed, welding speed, axial force, tool shoulder diameter, pin diameter, and tool hardness	Tensile strength
[18]	2017	Al5052-H32 alloy	Response surface methodology	Tool profile, rotational speed, welding speed, and tool tilt angle	Tensile strength and elongation
[19]	2012	Dissimilar alloy: AA6061-T6 and AA7075-T6	Response surface methodology	Rotational speed, welding speed, and axial force	Ultimate tensile strength, yield strength, and displacement
[20]	2009	Cast aluminum alloy A319	Taguchi method and analysis of variance (ANOVA)	Tool rotation speed, welding speed, and axial force	Tensile strength
[21]	2021	Dissimilar aluminum alloys 6061 and 5083	Response surface methodology	Tool pin profile, tool rotation speed, feed rate, and tool tilt angle	Ultimate tensile strength, yield strength, and microhardness
[22]	2021	Dissimilar AA7075-T651 and AA6061	Taguchi technique and analysis of variance (ANOVA)	Tool offset, pin profile of tool, and tilt angle of tool	Tensile strength
[23]	2022	Armor-grade aluminum alloys AA5083	Response surface methodology, regression, and analysis of variance (ANOVA)	Shoulder diameter, shoulder flatness, pin profile, and welding speed	Ultimate and yield tensile strength and elongation

Table 1 continued

Reference	Year	Material	Method	Parameters	Objective
[24]	2021	Dissimilar aluminum alloys of AA 7075-O and AA 5052-O grade	Taguchi approach and analysis of variance (ANOVA)	Tool pin profile, tool rotational speed, feed rate, and tool offset	Tensile strength and microhardness
[25]	2018	Dissimilar AA5083-O and AA6063-T6 aluminum alloys	Artificial intelligence and genetic algorithm	Tool rotational speed, welding speed, shoulder diameter, and pin diameter	Tensile strength, microhardness, and grain size
[26]	2021	Dissimilar AA3103 and AA7075 aluminum alloys	Taguchi method	Tool rotation speed, feed rate, and tool pin profile	Hardness, tensile strength, and impact strength
[27]	2018	Armor-marine grade AA7039	Desirability approach: RSM & ANOVA	Rotational speed, feed rate, and tilt angle	Ultimate tensile strength and tensile elongation

In the FSW, a tool moves along the joint line of two plates (similar or dissimilar) that simultaneously rotates and therefore it creates frictional heat that mechanically intermixes the metals and forges the hot and softened metal by the applied axial force. Figure 1 depicts the schematic of the FSW process and its effective parameters such as axial force, rotational and traverse speeds as well as tool geometry and hardness. As mentioned, in the FSW both mechanical and thermal processes are involved which show their effects in the welding zone and its surrounding regions and divide it into four major parts of Weld Nugget (WN), Thermo-Mechanically Affected Zone (TMAZ), Heat Affected Zone (HAZ), and Base Material (BM) that can be described as fully recrystallized region, area that plastically deformed without recrystallization, thermal affected, and region of original properties, respectively [36]. Because of the variety of physical phenomena in the FSW process, its analysis and optimization have become very complicated. Therefore, scholars have tried to solve the problems in this field by considering different alternative approaches of experiments like modeling and optimization methods [37]. In this regard, chu et al. have performed mechanical and microstructural optimization in the FSW joint of Al-Li alloy [38]. They used RSM and Box-Behnken experimental design to maximize static strength (i.e., tensile and shear stresses). Moreover, Electron Backscattering Diffraction (EBSD) and Differential Scanning Calorimetry (DSC) observations have been utilized to optimize hardness and reach the ultrafine grains. Sreenivasan et al. have optimized FSW process parameters for joining composite materials (i.e., AA7075 - SiC) [39]. They considered different parameters, including friction pressure, spindle speed, burn-off length, and upset pressure, in three levels, as the input variables in the optimization algorithms. Also, they tried to optimize hardness and Ultimate Tensile Strength (UTS). To achieve this goal, they employed two methods of linear regression and genetic algorithm. In a similar study, FSW process parameters have been opti-

mized to obtain the maximum joint strength and the highest elongation [40]. Also, Heidarzadeh et al. have employed ANOVA and RSM analysis to present mathematical relationships between the strength, elongation, and hardness of the connection in terms of FSW process parameters, including rotation speed, traverse speed, and axial force. They stated that the hardness reduces by raising the rotation speed and axial force and decreasing the traverse speed at the same time. Moreover, rotation speed and axial force are the most important factors that affect the strength and elongation values, respectively. After that, Heidarzadeh continued his research in this field with a focus on material properties and imaging observations, including EBSD and TEM [41]. He et al. have published a review report on the numerical simulation of FSW process [42]. They discussed different techniques for process simulation and presented the results obtained from them. However, methods based on artificial intelligence such as neural networks are remarkably applied in different aspects of science and engineering [43-46] as well as their application for modeling of FSW process [47-49]. In general, a neural network has three major layers of input, hidden, and output [50,51]. A literature review conducted in this research shows that shallow Neural Network (SNN), as the primary generation of artificial neural networks, has been mostly used in the simulation of FSW. In fact, SNNs have 1 or 2 hidden layers which are generally trained by Back-Propagation (BP) algorithm [46]. These networks besides their beneficial applications have some limitations. The most important limitation of SNNs is that a large number of data sets are required for their development. Recently, by considering the improvements achieved in the training of neural networks by deep learning presented by Hinton et al. [52], it is feasible to develop deep neural network with higher efficiency by employing small data set [53]. As an innovation, the current paper aims to show the capability of the DNN for prediction, analysis, and optimization of the FSW process for the first time by using small data

set. In the following, the authors have attempted to assess strength and hardness in the welded zone in terms of different process parameters as well as pin and shoulder features (i.e., hardness and diameter).

2. Experimental Data

The data used in this research were extracted from the paper published by Rajakumar et al. [54]. In order to conduct experiments, they prepared rolled sheets of 7075-T6 aluminum alloy with a thickness of 5 mm and dimensions of 150 × 300 mm. The ultimate and yield tensile strengths of the sheets are 485 and 410 MPa, respectively. Table 2

also presents the chemical composition of this material. Next, friction stir welding operation perpendicular to the rolling was performed as a single pulse and with non-consumable tools. The details of this process are shown in Figure 2.

In the next step, tensile test samples were fabricated according to the ASTM standard. They prepared two types of smooth and notched samples. All tests were performed at room temperature and at a speed of 0.5 mm/min. However, in the present study, only the laboratory results for smooth samples were used. Moreover, Vickers microhardness in the welded zone was measured by applying a force of 50 gr.

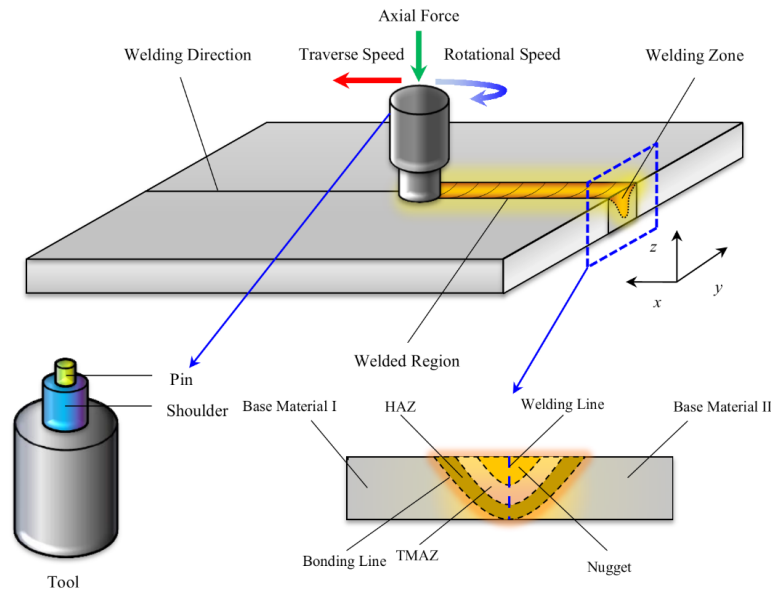


Figure 1. Schematic illustration of the FSW process and parameters affecting welded joint quality.

Table 2. Chemical composition of prepared sheets.

Element	Mg	Mn	Zn	Fe	Cu	Si	Al
Value (%)	2.10	0.12	5.10	0.35	1.2	0.58	90.55

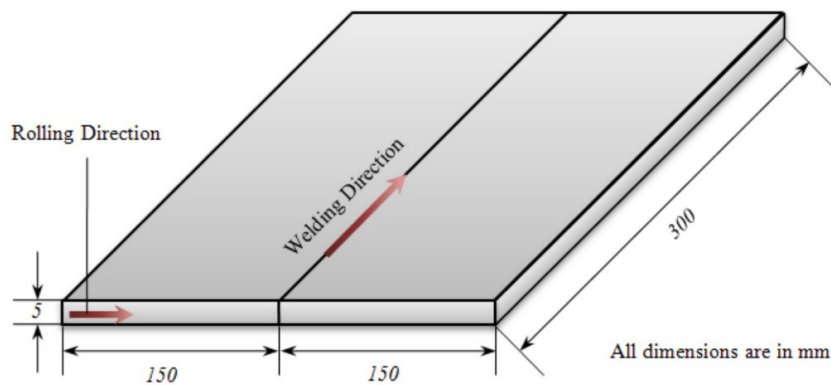


Figure 2. Dimensional details of sheets, sheets rolling and welding process directions.

3. DNN Developing

A DNN with four hidden layers was developed to model the FSW process by using experimental data described in the previous section. This experimental dataset was selected because it includes high amounts of effective parameters of FSW process. Nevertheless, the data used for this simulation is given in the Appendix (Table A1). Also, the first author has used these data previously for providing a model based on the common SNN with BP method [48]. Hence, the innovation of the present work with the previous one is to present a novel modified neural network based on deep learning. Parameters of axial force, rotational and traverse speeds as well as shoulder and pin diameters, and tool hardness were considered to investigate their related influences on the strength and

used for the training and testing steps, respectively. In addition, in order to develop DNN, as the dataset is small, a Stacked Auto-Encoder (SAE) was used for pre-training of DNN. SAE is a specific hidden layer SNN that has the same input and output layers and also has the same number of neurons in each layer of it with respect to the main DNN architecture. Used DNN along with linking to SAE is presented in Figure 3. Also, the accuracy of predicted results was determined via correlation coefficient (R2). The obtained accuracies for the developed DNN with and without SAE for both training and testing steps based on equation (1) are reported in Table 3.

$$R = \frac{\sum_{i=1}^n (f_{EXP,i} - \bar{F}_{EXP})(f_{DNN,i} - \bar{F}_{DNN})}{\sqrt{\sum_{i=1}^n ((f_{EXP,i} - \bar{F}_{EXP})^2 (f_{DNN,i} - \bar{F}_{DNN})^2)}} \quad (1)$$

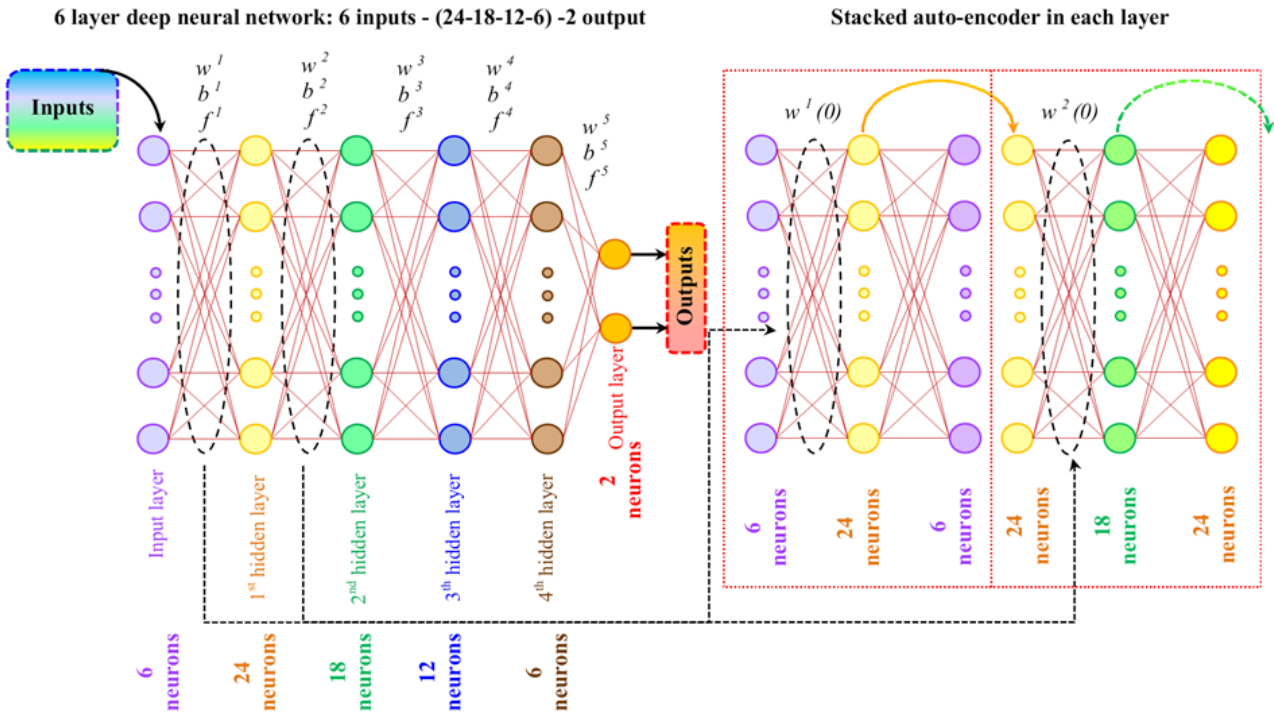


Figure 3. Used DNN along with linking to SAE.

Table 3. Obtained values of accuracies for developed DNN.

Developed DNN	Accuracy
Without SAE-train	0.982
Without SAE-test	0.974
With SAE-train	0.996
With SAE-test	0.993

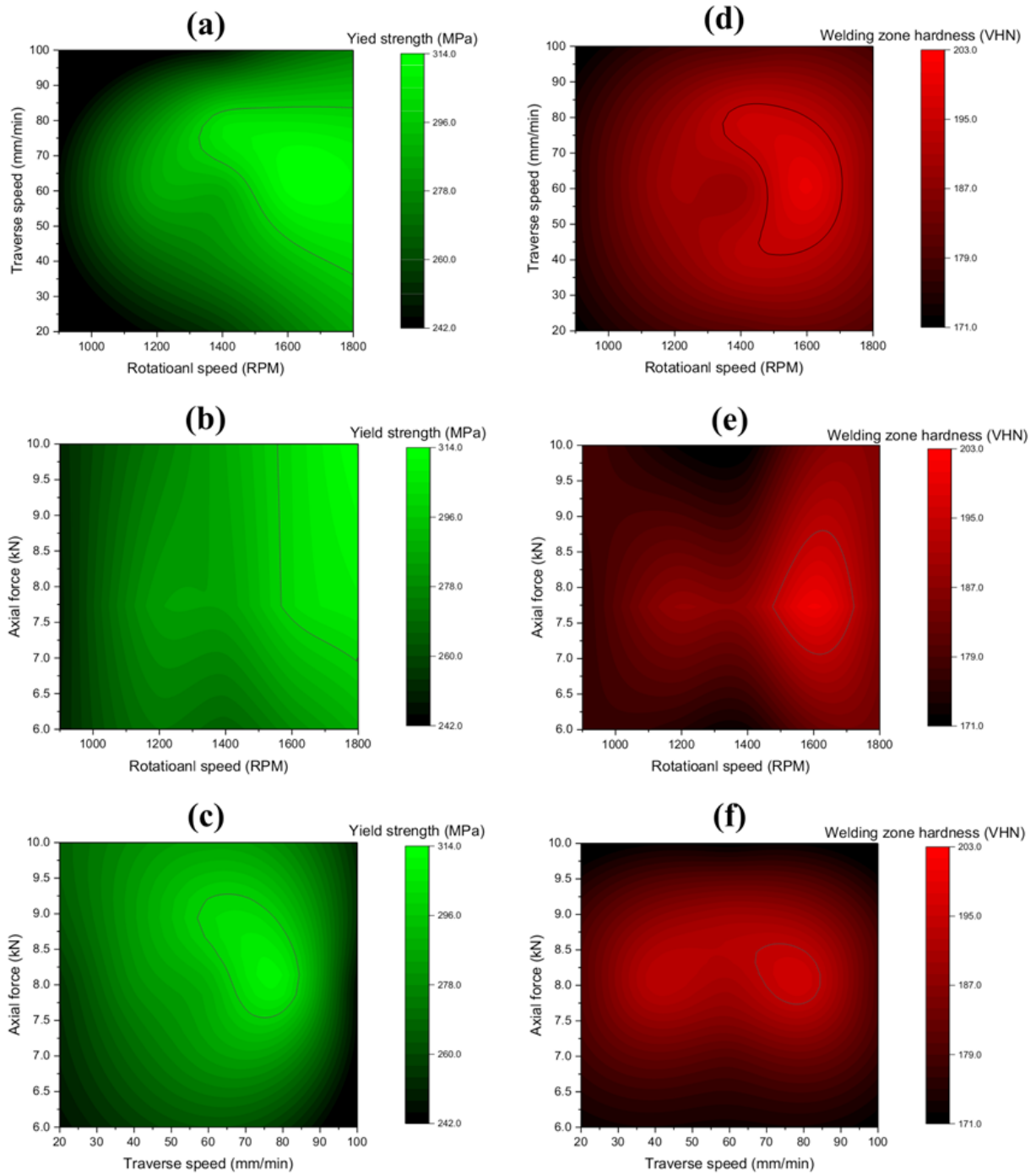
4. Results and Discussions

Based on the results of the determination of accuracies that show the DNN was developed well, parametric analysis was performed. In Figure 4 and Figure 5, the effects of welding process parameters and tool features on the welded zone strength and hardness are continuously revealed respectively in a general condition and interval of each parameter for the applied analyses are shown at the bottom of each contour. The region that has $\leq 95\%$ of the considered experimental value was specified in each 2D contour by a black line. It can be seen that, in the same graph whole prediction, analysis, and optimization can be carried out with accuracy close to 100% ($R^2 \approx 1$). From Figure 4, as the rotation speed increases, the strength of the welded zone always increases, which is consistent with the results of Ahmed et al. in the study of 2022^[33]. Also, with the increase of the axial force, the strength improves, but its changes are not significant compared to the rotational speed parameter and it depends on the values of other parameters. Ref No. 33 also deals with the optimization of process parameters. The authors showed that the tensile strength of FSW joint considering the feed rate of 18 mm/min is much higher than the tensile strength of FSW joint with feed rates of 16 and 20 mm/min. In other words, the tensile strength of the connection increases with the increase of the feed rate in the range of 16 to 18 mm/min, and it decreases with the increase of the feed rate in the range of 18 to 20 mm/min. Therefore, this interpretation is exactly in accordance with the results presented in Figure 4. Moreover, the contour presented in Figure 4b indicates that if the rotational speed is less than 1000 rpm, changes in axial force do not affect the strength. However, all the results presented in this section are considering the welding conditions in this study and different results may be obtained in other conditions. Therefore, more studies are needed to generalize the results to other conditions,

which is on the agenda of this research group for its future studies. Furthermore, by focusing on the hardness in the welded zone as a response, it is seen that the hardness increases with increasing rotational speed. But in interaction with other parameters, i.e., axial force and transverse speed, there is an intermediate area where the highest hardness is obtained within this specific area and the lowest hardness is obtained outside this area. For example, it is clear from Figure 4f that setting the rotational speed in the range of 1500 to 1700 rpm and also the axial force between 7 and 9 KN can result in the highest hardness in the welded zone.

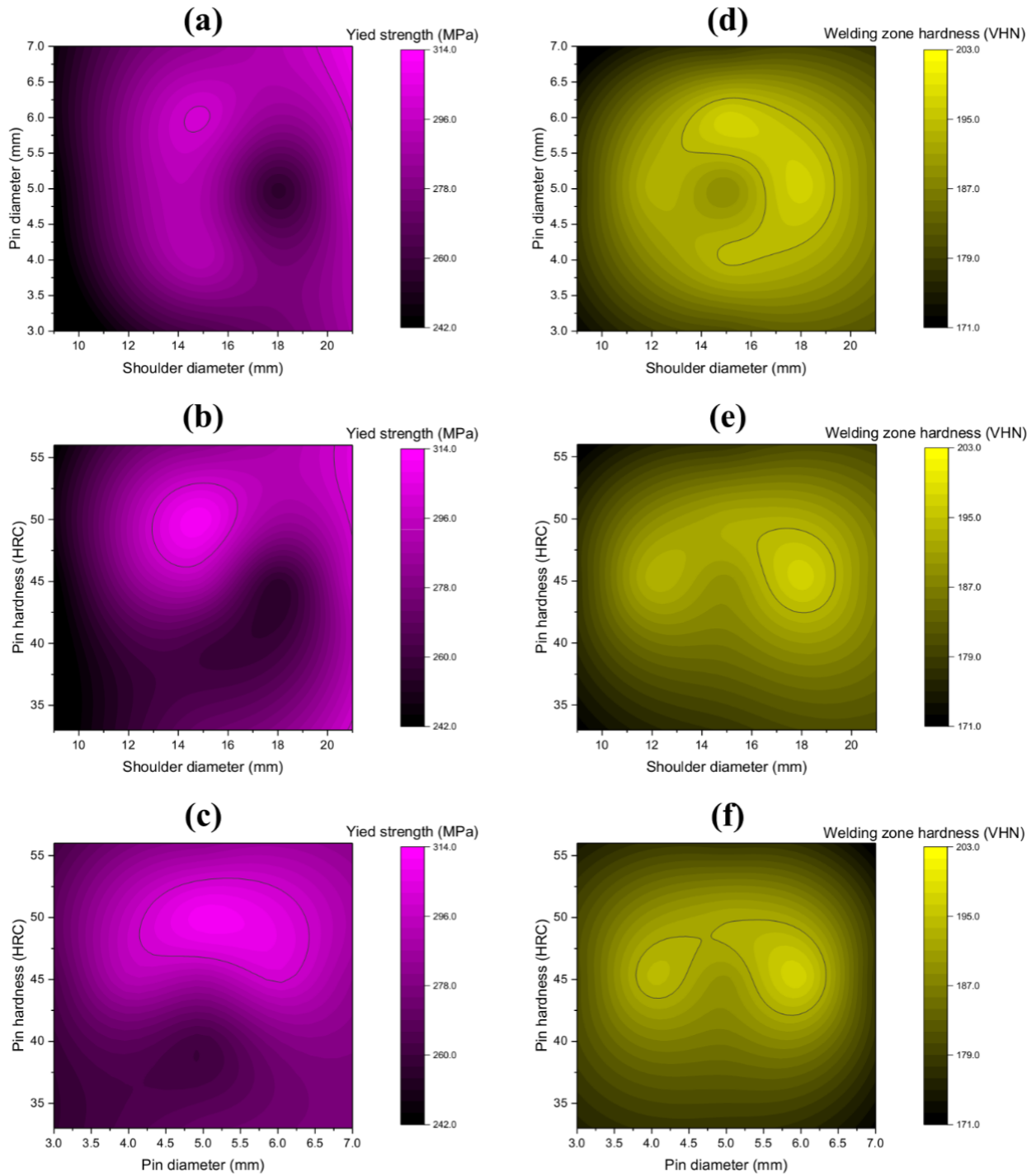
As shown in Figure 5, no specific trends can be found between the system responses (i.e., strength and hardness in the welded zone) and tool characteristics, including pin and shoulder diameters and their hardness. In other words, the interaction between various parameters of this section must be checked with more precision and laboratory data and it is very difficult and perhaps unlikely to be able to independently declare the effect of one of these parameters on the output, because depending on the conditions of other parameters, there is a possibility of changing the state of the response. It is clearly evident in the contours with yellow color theme (i.e., Figure 5d, e, and f) that there are different circular and elliptical layers, therefore, there is a specific area in each contour that should be tried to select the characteristics of the tool in such a way that the responses be placed within these areas.

In summary, according to all the achievements presented above, in order to obtain the optimal parameters, all the contours should be placed on each other at the same time and the common space between the areas marked by black lines should be selected. In this way, optimal values of rotational speed, traverse speed, axial force, shoulder diameter, pin diameter, and tool hardness are specified as 1600 rpm, 65 mm/min, 8 KN, 15.5 mm, 5.75 mm, and 50 HRC, respectively.



$$9 \leq \text{Shoulder diameter} \leq 21, 3 \leq \text{Pin diameter} \leq 7, 33 \leq \text{tool hardness} \leq 56$$

Figure 4. Parametric analysis of the effects of axial force, rotational and traverse speeds on strength (a-c) and hardness (d-f) of welded zone.



$900 \leq \text{Rotational speed} \leq 1800$, $20 \leq \text{Traverse speed} \leq 100$, $6 \leq \text{Axial force} \leq 10$

Figure 5. Parametric analysis of the effects of shoulder diameter, pin diameter, and tool hardness on strength (a-c) and hardness (d-f) of welded zone.

5. Conclusions

The application of DNN to model the FSW process was investigated in this study. The obtained results revealed that by using SAE for pre-training of neural networks higher accuracy can be obtained. In addition, it can be concluded that by applying DNN on small dataset with discrete values, continuous values for whole considered intervals can be predicted for parametric analysis of FSW. Moreover, these 2D contours with the accuracy of close to 100% can be easily used for further analysis and optimization. However, one of the challenges in this research was that the small dataset was used to estimate the tensile strength, but more studies are needed to optimize the hardness, and no specific trend was found for hardness changes in the welded area according to the investigated parameters. Therefore, in future research, the authors seek to perform more tests using design of experiment (DOE) techniques such as Taguchi method and considering more input parameters. In addition, the authors agree with the opinion of many reports that the main causes of failures of mechanical parts are the fatigue phenomenon^[55]. Therefore, in the future research series, this research team seeks to model, analyse, and optimize the friction stir welding process of aluminium sheets with the aim of improving the fatigue life of the joint. For this, they will use various techniques including data mining, artificial intelligence, deep learning, etc. to make a comprehensive study. Also, the accuracy of the methods will be compared with each other and the advantages and disadvantages of each of them will be discussed.

Author Contributions

Conceptualization, E.M., O.U., and K.R.K.; methodology, E.M., O.U., S.M.S.S., and K.R.K.; software, E.M., O.U., and S.M.S.S.; validation, E.M., and O.U.; formal analysis, E.M., O.U., and K.R.K.; investigation, E.M., O.U., S.M.S.S., K.R.K., and N.A.; resources, E.M., O.U., and K.R.K.; data curation, E.M., and O.U.; writing—original draft preparation, E.M., O.U., S.M.S.S., and K.R.K.; writing—review and editing, K.R.K.; visualization, E.M., O.U., and K.R.K.; supervision, E.M., O.U., and K.R.K.; project administration, E.M., and K.R.K.; funding acquisition, E.M., O.U., and K.R.K., All authors have read and agreed to the published version of the manuscript.

Funding

This research received no external funding.

Acknowledgement

This paper has been supported by the RUDN Universi-

ty Strategic Academic Leadership Program.

Data Availability

The data that support the findings of this study are available from the corresponding author upon reasonable request.

Conflict of Interest

The authors declare no conflict of interest.

References

- [1] Gite, R.A., Loharkar, P.K., Shimpi, R., 2019. Friction stir welding parameters and application: A review. *Materials Today: Proceedings*. 19, 361-365. DOI: <https://doi.org/10.1016/j.matpr.2019.07.613>
- [2] Reza Kashyzadeh, K., Ghorbani, S., 2023. High-cycle fatigue behavior and chemical composition empirical relationship of low carbon three-sheet spot-welded joint: An application in automotive industry. *Journal of Design Against Fatigue*. 2(1), 1-8.
- [3] Amiri, N., Farrahi, G.H., Kashyzadeh, K.R., et al., 2020. Applications of ultrasonic testing and machine learning methods to predict the static & fatigue behavior of spot-welded joints. *Journal of Manufacturing Processes*. 52, 26-34.
- [4] Reza Kashyzadeh, K., Farrahi, G., Ahmadi, A., et al., 2023. Fatigue life analysis in the residual stress field due to resistance spot welding process considering different sheet thicknesses and dissimilar electrode geometries. *Proceedings of the Institution of Mechanical Engineers, Part L: Journal of Materials: Design and Applications*. 237(1), 33-51. DOI: <https://doi.org/10.1177/14644207221101069>
- [5] Farrahi, G.H., Ahmadi, A., Kashyzadeh, K.R., 2020. Simulation of vehicle body spot weld failures due to fatigue by considering road roughness and vehicle velocity. *Simulation Modelling Practice and Theory*. 105, 102168. DOI: <https://doi.org/10.1016/j.simpat.2020.102168>
- [6] Farrahi, G.H., Ahmadi, A., Kashyzadeh, K.R., et al., 2020. A comparative study on the fatigue life of the vehicle body spot welds using different numerical techniques: Inertia relief and Modal dynamic analyses. *Frattura ed Integrità Strutturale*. 14(52), 67-81. DOI: <https://doi.org/10.3221/IGF-ESIS.52.06>
- [7] Farrahi, G.H., Kashyzadeh, K.R., Minaei, M., et al., 2020. Analysis of resistance spot welding process parameters effect on the weld quality of three-steel sheets used in automotive industry: Experimental and finite element simulation. *International Journal of Engineering*. 33(1), 148-157.

- DOI: <https://doi.org/10.5829/ije.2020.33.01a.17>
- [8] Friction Stir Butt Welding, International Patent Application No. PCT/GB92 [Internet]. International Patent Application No. PCT/GB92. GB Patent Application No. 9125978.8. Available from: <https://cir.nii.ac.jp/crid/1570291224176390272>
- [9] Roldo, L., Vulić, N., 2019. Friction stir welding for marine applications: mechanical behaviour and microstructural characteristics of Al-Mg-Si-Cu plates. *Transactions on Maritime Science*. 8(1), 75-83. DOI: <https://doi.org/10.7225/toms.v08.n01.008>
- [10] Silva, A.C., Braga, D.F., De Figueiredo, M.A.V., et al., 2015. Ultimate tensile strength optimization of different FSW aluminium alloy joints. *The International Journal of Advanced Manufacturing Technology*. 79, 805-814. DOI: <https://doi.org/10.1007/s00170-015-6871-2>
- [11] Aydin, H., Bayram, A., Esme, U., et al., 2010. Application of grey relation analysis (GRA) and Taguchi method for the parametric optimization of friction stir welding (FSW) process. *Materials and Technology*. 44(4), 205-211.
- [12] Ghetiyya, N.D., Patel, K.M., Kavar, A.J., 2016. Multi-objective optimization of FSW process parameters of aluminium alloy using Taguchi-based grey relational analysis. *Transactions of the Indian Institute of Metals*. 69, 917-923. DOI: <https://doi.org/10.1007/s12666-015-0581-1>
- [13] Deepandurai, K., Parameshwaran, R., 2016. Multi-response optimization of FSW parameters for cast AA7075/SiCp composite. *Materials and Manufacturing Processes*. 31(10), 1333-1341. DOI: <https://doi.org/10.1080/10426914.2015.1117628>
- [14] Bhushan, R.K., Sharma, D., 2019. Optimization of FSW parameters for maximum UTS of AA6082/SiC/10P composites. *Advanced Composites Letters*. 28, 0963693519867707. DOI: <https://doi.org/10.1177/0963693519867707>
- [15] Jain, S., Sharma, N., Gupta, R., 2018. Dissimilar alloys (AA6082/AA5083) joining by FSW and parametric optimization using Taguchi, grey relational and weight method. *Engineering Solid Mechanics*. 6(1), 51-66. DOI: <http://dx.doi.org/10.5267/j.esm.2017.10.003>
- [16] Lakshminarayanan, A.K., Balasubramanian, V., 2008. Process parameters optimization for friction stir welding of RDE-40 aluminium alloy using Taguchi technique. *Transactions of Nonferrous Metals Society of China*. 18(3), 548-554. DOI: [https://doi.org/10.1016/S1003-6326\(08\)60096-5](https://doi.org/10.1016/S1003-6326(08)60096-5)
- [17] Rajakumar, S., Muralidharan, C., Balasubramanian, V., 2010. Optimization of the friction-stir-welding process and tool parameters to attain a maximum tensile strength of AA7075-T6 aluminium alloy. *Proceedings of the Institution of Mechanical Engineers, Part B: Journal of Engineering Manufacture*. 224(8), 1175-1191. DOI: <https://doi.org/10.1243/09544054JEM1802>
- [18] Shanavas, S., Dhas, J.E.R., 2017. Parametric optimization of friction stir welding parameters of marine grade aluminium alloy using response surface methodology. *Transactions of Nonferrous Metals Society of China*. 27(11), 2334-2344. DOI: [https://doi.org/10.1016/S1003-6326\(17\)60259-0](https://doi.org/10.1016/S1003-6326(17)60259-0)
- [19] Elatharasan, G., Kumar, V.S., 2012. Modelling and optimization of friction stir welding parameters for dissimilar aluminium alloys using RSM. *Procedia Engineering*. 38, 3477-3481. DOI: <https://doi.org/10.1016/j.proeng.2012.06.401>
- [20] Jayaraman, M., Sivasubramanian, R., Balasubramanian, V., et al., 2009. Optimization of Process Parameters for Friction Stir Welding of Cast Aluminium Alloy A319 by Taguchi Method [Internet]. Available from: <http://nopr.nispr.res.in/handle/123456789/2786>
- [21] Verma, S., Kumar, V., 2021. Optimization of friction stir welding parameters of dissimilar aluminium alloys 6061 and 5083 by using response surface methodology. *Proceedings of the Institution of Mechanical Engineers, Part C: Journal of Mechanical Engineering Science*. 235(23), 7009-7020. DOI: <https://doi.org/10.1177/09544062211005804>
- [22] Yuvaraj, K.P., Varthanan, P.A., Haribabu, L., et al., 2021. Optimization of FSW tool parameters for joining dissimilar AA7075-T651 and AA6061 aluminium alloys using Taguchi Technique. *Materials Today: Proceedings*. 45, 919-925. DOI: <https://doi.org/10.1016/j.matpr.2020.02.942>
- [23] Ghangas, G., Singhal, S., Dixit, S., et al., 2022. Mathematical modeling and optimization of friction stir welding process parameters for armor-grade aluminium alloy. *International Journal on Interactive Design and Manufacturing (IJIDeM)*. 1-18. DOI: <https://doi.org/10.1007/s12008-022-01000-1>
- [24] Ramesha, K., Sudersanan, P.D., Santhosh, N., et al., 2021. Design and optimization of the process parameters for friction stir welding of dissimilar aluminium alloys. *Engineering and Applied Science Research*. 48(3), 257-267.
- [25] Gupta, S.K., Pandey, K.N., Kumar, R., 2018. Artificial intelligence-based modelling and multi-objective optimization of friction stir welding of dissimilar

- AA5083-O and AA6063-T6 aluminium alloys. Proceedings of the Institution of Mechanical Engineers, Part L: Journal of Materials: Design and Applications. 232(4), 333-342.
DOI: <https://doi.org/10.1177/1464420715627293>
- [26] Raj, A., Kumar, J.P., Rego, A.M., et al., 2021. Optimization of friction stir welding parameters during joining of AA3103 and AA7075 aluminium alloys using Taguchi method. *Materials Today: Proceedings*. 46, 7733-7739.
DOI: <https://doi.org/10.1016/j.matpr.2021.02.246>
- [27] Verma, S., Gupta, M., Misra, J.P., 2018. Optimization of process parameters in friction stir welding of armor-marine grade aluminium alloy using desirability approach. *Materials Research Express*. 6(2), 026505.
DOI: <https://doi.org/10.1088/2053-1591/aaea01>
- [28] Maleki, E., Unal, O., Seyedi Sahebari, S.M., et al., 2023. A novel approach for analyzing the effects of almen intensity on the residual stress and hardness of shot-peened (TiB+ TiC)/Ti-6Al-4V composite: Deep learning. *Materials*. 16(13), 4693.
DOI: <https://doi.org/10.3390/ma16134693>
- [29] Maleki, E., Unal, O., Seyedi Sahebari, S.M., et al., 2022. Application of deep neural network to predict the high-cycle fatigue life of AISI 1045 steel coated by industrial coatings. *Journal of Marine Science and Engineering*. 10(2), 128.
DOI: <https://doi.org/10.3390/jmse10020128>
- [30] Padhy, G.K., Wu, C.S., Gao, S., 2018. Friction stir based welding and processing technologies-processes, parameters, microstructures and applications: A review. *Journal of Materials Science & Technology*. 34(1), 1-38.
DOI: <https://doi.org/10.1016/j.jmst.2017.11.029>
- [31] Gangwar, K., Ramulu, M., 2018. Friction stir welding of titanium alloys: A review. *Materials & Design*. 141, 230-255.
DOI: <https://doi.org/10.1016/j.matdes.2017.12.033>
- [32] Mohanty, H.K., Mahapatra, M.M., Kumar, P., et al., 2012. Modeling the effects of tool shoulder and probe profile geometries on friction stirred aluminum welds using response surface methodology. *Journal of Marine Science and Application*. 11, 493-503.
DOI: <https://doi.org/10.1007/s11804-012-1160-z>
- [33] Ahmed, S., Rahman, R.A.U., Awan, A., et al., 2020. Optimization of process parameters in friction stir welding of aluminum 5451 in marine applications. *Journal of Marine Science and Engineering*. 10(10), 1539.
DOI: <https://doi.org/10.3390/jmse10101539>
- [34] Kumar, D.A., Biswas, P., Tikader, S., et al., 2013. A study on friction stir welding of 12mm thick aluminum alloy plates. *Journal of Marine Science and Application*. 12, 493-499.
DOI: <https://doi.org/10.1007/s11804-013-1221-y>
- [35] Ganjabi, M.A., Farrahi, G., Reza Kashyzadeh, K., et al., 2023. Effects of various strength defects of spot weld on the connection strength under both static and cyclic loading conditions: empirical and numerical investigation. *The International Journal of Advanced Manufacturing Technology*. 127, 5665-5678.
DOI: <https://doi.org/10.1007/s00170-023-11923-y>
- [36] Boukraa, M., Lebaal, N., Mataoui, A., et al., 2018. Friction stir welding process improvement through coupling an optimization procedure and three-dimensional transient heat transfer numerical analysis. *Journal of Manufacturing Processes*. 34, 566-578.
DOI: <https://doi.org/10.1016/j.jmapro.2018.07.002>
- [37] Heidarzadeh, A., Chabok, A., Pei, Y., 2019. Friction stir welding of Monel alloy at different heat input conditions: Microstructural mechanisms and tensile behavior. *Materials Letters*. 245, 94-97.
DOI: <https://doi.org/10.1016/j.matlet.2019.02.108>
- [38] Chu, Q., Li, W.Y., Yang, X.W., et al., 2018. Microstructure and mechanical optimization of probeless friction stir spot welded joint of an Al-Li alloy. *Journal of Materials Science & Technology*. 34(10), 1739-1746.
DOI: <https://doi.org/10.1016/j.jmst.2018.03.009>
- [39] Sreenivasan, K.S., Kumar, S.S., Katiravan, J., 2019. Genetic algorithm based optimization of friction welding process parameters on AA7075-SiC composite. *Engineering Science and Technology, an International Journal*. 22(4), 1136-1148.
DOI: <https://doi.org/10.1016/j.jestch.2019.02.010>
- [40] Heidarzadeh, A., Barenji, R.V., Khalili, V., et al., 2019. Optimizing the friction stir welding of the α/β brass plates to obtain the highest strength and elongation. *Vacuum*. 159, 152-160.
DOI: <https://doi.org/10.1016/j.vacuum.2018.10.036>
- [41] Heidarzadeh, A., 2019. Tensile behavior, microstructure, and substructure of the friction stir welded 70/30 brass joints: RSM, EBSD, and TEM study. *Archives of Civil and Mechanical Engineering*. 19(1), 137-146.
DOI: <https://doi.org/10.1016/j.acme.2018.09.009>
- [42] He, X., Gu, F., Ball, A., 2014. A review of numerical analysis of friction stir welding. *Progress in Materials Science*. 65, 1-66.
DOI: <https://doi.org/10.1016/j.pmatsci.2014.03.003>
- [43] Maleki, E., Bagherifard, S., Razavi, S.M.J., et al., 2022. On the efficiency of machine learning for fa-

tigue assessment of post-processed additively manufactured AlSi10Mg. *International Journal of Fatigue*. 160, 106841.
DOI: <https://doi.org/10.1016/j.ijfatigue.2022.106841>

[44] Maleki, E., Unal, O., Kashyzadeh, K.R., 2019. Surface layer nanocrystallization of carbon steels subjected to severe shot peening: Analysis and optimization. *Materials Characterization*. 157, 109877.
DOI: <https://doi.org/10.1016/j.matchar.2019.109877>

[45] Maleki, E., Unal, O., Kashyzadeh, K.R., 2018. Fatigue behavior prediction and analysis of shot peened mild carbon steels. *International Journal of Fatigue*. 116, 48-67.
DOI: <https://doi.org/10.1016/j.ijfatigue.2018.06.004>

[46] Reza Kashyzadeh, K., Amiri, N., Ghorbani, S., et al., 2022. Prediction of concrete compressive strength using a back-propagation neural network optimized by a genetic algorithm and response surface analysis considering the appearance of aggregates and curing conditions. *Buildings*. 12(4), 438.
DOI: <https://doi.org/10.3390/buildings12040438>

[47] Dewan, M.W., Huggett, D.J., Liao, T.W., et al., 2016. Prediction of tensile strength of friction stir weld joints with adaptive neuro-fuzzy inference system (ANFIS) and neural network. *Materials & Design*. 92, 288-299.
DOI: <https://doi.org/10.1016/j.matdes.2015.12.005>

[48] Maleki, E., 2015. Artificial neural networks application for modeling of friction stir welding effects on mechanical properties of 7075-T6 aluminum alloy. *IOP Conference Series: Materials Science and Engineering*. 103(1), 012034.
DOI: <https://doi.org/10.1088/1757-899X/103/1/012034>

[49] Shojaeefard, M.H., Behnagh, R.A., Akbari, M., et al., 2013. Modelling and Pareto optimization of mechanical properties of friction stir welded AA7075/AA5083 butt joints using neural network and particle swarm algorithm. *Materials & Design*. 44, 190-198.
DOI: <https://doi.org/10.1016/j.matdes.2012.07.025>

[50] Maleki, E., Bagherifard, S., Guagliano, M., 2022. Application of artificial intelligence to optimize the process parameters effects on tensile properties of Ti-6Al-4V fabricated by laser powder-bed fusion. *International Journal of Mechanics and Materials in Design*. 18(1), 199-222.
DOI: <https://doi.org/10.1007/s10999-021-09570-w>

[51] Kashyzadeh, K.R., Ghorbani, S., 2023. New neural network-based algorithm for predicting fatigue life of aluminum alloys in terms of machining parameters. *Engineering Failure Analysis*. 146, 107128.
DOI: <https://doi.org/10.1016/j.engfailanal.2023.107128>

[52] Hinton, G.E., Osindero, S., Teh, Y.W., 2006. A fast learning algorithm for deep belief nets. *Neural Computation*. 18(7), 1527-1554.
DOI: <https://doi.org/10.1162/neco.2006.18.7.1527>

[53] Feng, S., Zhou, H., Dong, H., 2019. Using deep neural network with small dataset to predict material defects. *Materials & Design*. 162, 300-310.
DOI: <https://doi.org/10.1016/j.matdes.2018.11.060>

[54] Rajakumar, S., Muralidharan, C., Balasubramanian, V., 2011. Influence of friction stir welding process and tool parameters on strength properties of AA7075-T6 aluminium alloy joints. *Materials & Design*. 32(2), 535-549.
DOI: <https://doi.org/10.1016/j.matdes.2010.08.025>

[55] Arghavan, A., Reza Kashyzadeh, K., Asfarjani, A.A., 2011. Investigating effect of industrial coatings on fatigue damage. *Applied Mechanics and Materials*. 87, 230-237.
DOI: <https://doi.org/10.4028/www.scientific.net/AMM.87.230>

Appendix A

The data used in this research, including various welding conditions and laboratory results of tensile and microhardness tests, are given in Table A1.

Table A1. The data used in the current study, including welding conditions and testing results.

Case No.	FSW Process Parameters			Tool Features			Responses in Welded Zone	
	Rotational speed (rpm)	Transverse speed (mm/min)	Axial force (KN)	Shoulder diameter (mm)	Pin diameter (mm)	Tool hardness (HRc)	Strength (MPa)	Hardness (VHN)
1	1400	60	8	15	5	45	314	203
2	1800	60	8	15	5	45	310	185
3	1400	40	8	15	5	45	279	194
4	1400	60	8	15	5	45	310	198
5	1400	80	8	15	5	45	308	197
6	1400	60	7	15	5	45	282	180
7	1400	60	8	15	5	45	314	199

Table A1 continued

Case No.	FSW Process Parameters			Tool Features			Responses in Welded Zone	
	Rotational speed (rpm)	Transverse speed (mm/min)	Axial force (KN)	Shoulder diameter (mm)	Pin diameter (mm)	Tool hardness (HRc)	Strength (MPa)	Hardness (VHN)
8	1400	60	8	12	5	45	280	193
9	1400	60	8	15	5	45	310	198
10	1400	60	8	18	5	45	256	197
11	1400	60	8	15	4	45	292	194
12	1400	60	8	15	5	45	310	198
13	1400	60	8	15	6	45	300	197
14	1400	60	8	15	5	40	261	186
15	1400	60	8	15	5	45	313	198
16	900	60	8	15	5	45	245	175
17	1200	60	8	15	5	45	290	191
18	1400	20	8	15	5	45	255	180
19	1400	100	8	15	5	45	245	179
20	1400	60	6	15	5	45	263	173
21	1400	60	10	15	5	45	285	171
22	1400	60	8	9	5	45	242	178
23	1400	60	8	21	5	45	296	187
24	1400	60	8	15	3	45	264	181
25	1400	60	8	15	7	45	284	178
26	1400	60	8	15	5	33	271	178
27	1400	60	8	15	5	56	282	178
28	1400	60	9	15	5	45	301	190
29	1400	60	8	15	5	50	310	192
30	1600	60	8	15	5	45	314	202

Source: Maleki, E., 2015^[48].